Changes in molecular dynamics of apomyoglobin during amyloid formation

2012 J. Phys.: Conf. Ser. 340 012092

(http://iopscience.iop.org/1742-6596/340/1/012092)

Journal of Physics: Conference Series **340** (2012) 012092 doi:10.1088/1742-6596/340/1/012092

Changes in molecular dynamics of apomyoglobin during amyloid formation

Andreas Maximilian Stadler [1,*], Elisa Fabiani [2], Giuseppe Zaccai [3]

[1] Forschungszentrum Jülich GmbH, ICS-1 & JCNS-1, 52425 Jülich, Germany

[2] Polytech'Grenoble - Université Joseph Fourier, BP 53, 38041 Grenoble Cedex 9 & Institut de Biologie Structurale J.P. Ebel, 41, rue Jules Horowitz, 38027 Grenoble Cedex 1

[3] Institut Laue-Langevin, 6 rue Jules Horowitz, 38042 Grenoble, France

*a.stadler@fz-juelich.de

Abstract. Changes of molecular dynamics associated with amyloid fibril formation were explored using apomyoglobin as a model system. Protein dynamics was measured using elastic incoherent neutron scattering. The formation of amyloid fibres was evidenced by the presence of characteristic signatures in the X-ray diffraction pattern.

1. Introduction

Many neurodegenerative diseases such as Alzheimer's and Parkinson's are correlated with protein misfolding, aggregation and deposition of insoluble amyloid fibers in cells and tissues [1, 2]. It is of both fundamental and medical interest to characterize the molecular reasons and connections of protein misfolding, aggregation and amyloid formation. Different classes of proteins are able to form amyloid fibers. One hypothesis states that it is even a general property of the polypeptide chain itself under destabilizing conditions such as extremes of heat or pH [1-3]. Amyloid fibers are densely packed with a high degree of structural order. A common diffraction pattern of amyloid fibers with two peaks at q = 0.62 and 1.36 Å^{-1} termed the cross-β pattern is characteristic of amyloid fibers [4]. The diffraction signature corresponds to the stacking distance of $d = 2\pi/q$ = 10.1 Å between different strands and to the characteristic repeat distance of d = 4.6 Å within β sheets.

Myoglobin (Mb) has served extensively as model system in molecular biophysics. Frauenfelder and co-workers called it once 'the hydrogen atom of biology' [5]. It is small enough to allow a fundamental understanding of the physical processes involved but sufficiently complex to represent typical protein behavior. The protein acts as a scaffold for a heme-group that can carry an oxygen molecule or other small ligands. The protein with heme-group is termed holo-Mb; without heme-group it is called apo-Mb. At temperatures above ~ 328 K (~ 55°C) and at basic solvent conditions of pH 9 apo-Mb is reported to form amyloid fibres [6, 7]. Disordered segments of apo-Mb that emerge at high temperature and conditions that are unfavorable for protein folding were found to be essential for amyloid fiber formation in apo-Mb [7].

We are using apo-Mb as a model system for the study of amyloid formation. Structural changes from the native-like α-helical state below 328 K to the β-sheet structure at temperatures above ~328 K have been monitored by small and wide angle X-ray scattering [8]. We have also studied the dynamics of apo- and holo-Mb during the α-to-β transition [9]. Using a simplified approach the results indicated a more resilient ("stiffer") β-sheet structure in apo-Mb at temperatures above ~328 K as compared to the native α-helical structure below ~ 328 K. However, we were not able to determine mean square displacements with sufficient accuracy to quantify changes in protein dynamics associated with amyloid formation and to deduce further information about protein resilience in absolute units.

In this article we report a study on changes in protein dynamics associated with amyloid formation. Elastic incoherent neutron scattering (EINS) was used to determine mean square displacements $\langle u^2 \rangle$ of protein thermal fluctuations with high accuracy. Thermal motions were investigated using two different neutron spectrometers with time resolutions of 0.1 and 1 ns, respectively. Effective force constants $\langle k' \rangle$ were calculated from the $\langle u^2 \rangle$ and are compared between the native state of apo-Mb during amyloid formation and of heat incubated apo-Mb which was shown to have characteristic signatures of amyloid fibers.

2. Material and Methods

2.1. Sample preparation

Horse heart Mb purchased from SIGMA-ALDRICH was dissolved in water. The pH of the Mb solution was then lowered to 1.5 with concentrated HCl on ice. The acidified solution was mixed with 4 volumes of 2-butanone. The upper organic layer was decanted, and the extraction was repeated twice. The aqueous layer was dialyzed against buffer solution (20 mM KH_2PO_4, pH 7) followed by pure water. After dialysis the protein solution was lyophilized to obtain apo-Mb powder.

For the neutron experiments, apo-Mb powder was hydrated by pipetting uniformly buffer solution (20 mM KH_2PO_4, pH 9) to the sample to a level of 0.73 g H_2O/g protein. This corresponds to approximately two hydration layers per protein and was intended to allow for some pH effects.

Around 120 mg hydrated protein powder was sealed in flat aluminum sample holders with internal spacing of 0.2 mm for the neutron scattering experiments. One sample was hermetically sealed in the sample holder and was incubated for 2 days at 338 K to promote the formation of amyloid fibers. The weight of the heat incubated sample was checked before and after the incubation time to ensure that no evaporation of hydration water occurred.

Small amounts of roughly 10 mg hydrated powder were measured in thin quartz tubes in the X-ray diffraction experiments. One hydrated powder sample was prepared at room temperature; the second sample was hermetically sealed and incubated at 338 K for 2 days to allow the formation of amyloid fibers, the third sample is a part of a sample which was measured on IN13 just before the X-ray experiments.

2.2. Elastic Incoherent Neutron Scattering

EINS is a well suited method for the study of the dynamics of complex biological macromolecules. Thermal and cold neutrons have wavelengths in the order of some Å and energies of some meV and are therefore sensitive probes to measure thermal molecular motions on an atomic length-scale and picosecond to nanosecond time-scale. In biological systems, the incoherent scattering is dominated by the signal of hydrogen atoms as their incoherent scattering cross section is much larger than that of the other elements that occur in biological matter [10]. In the time-scale of the neutron experiments, the H atoms reflect the motion of the chemical groups to which they are bound. As hydrogen atoms are uniformly distributed in proteins, neutron scattering detects average internal macromolecular motions. EINS experiments, so called 'elastic scans', provide the mean square displacements $\langle u^2 \rangle$ of the system as a function of temperature.

Mean square displacements $\langle u^2 \rangle$ were calculated within the Gaussian approximation according to

$$\left\langle u^2 \right\rangle = \frac{-6 \cdot \Delta(\ln I(q))}{\Delta q^2}, \quad (1)$$

where *I(q)* represents the measured elastic intensity and *q* the modulus of the scattering vector [11]. We use in this work the definition of $\langle u^2 \rangle$ introduced by Smith that accounts for the full amplitude of motions [12]. The Gaussian approximation is strictly valid for localized motions at $q^2 \to 0$ but holds up to $\left\langle u^2 \right\rangle \cdot q^2 \sim 2$ for motions with the most compact geometry. The validity of the approximation is similar to that of the Guinier region of small angle scattering, and depends on the geometry of the motion or the shape. Kidera and Go used normal mode refinement of X-ray crystallography data and showed that protein dynamics are intrinsically anisotropic with ellipoidal shape and axes of 1:1:1.7 [13]. For thermal motions with ellipsoidal axes of 1:1:~2 the Gaussian approximation holds to significantly larger values of roughly $\left\langle u^2 \right\rangle \cdot q^2 \sim 8$ as reported by Tehei et al. [14].

The temperature variation of the $\langle u^2 \rangle$ was interpreted in terms of an empirical effective force constant $\langle k' \rangle$ called resilience by Zaccai [15]

$$\left\langle k' \right\rangle = 0.00276 / \left(d \left\langle u^2 \right\rangle / dT \right). \quad (2)$$

The units are chosen such that $\langle k' \rangle$ is in N/m when $\langle u^2 \rangle$ is in Å^2 and *T* is in K [15]. The force constants describe the rigidity, or resilience, of the protein. Neutron scattering experiments

2.3. Neutron scattering experiments

EINS was measured on the neutron backscattering spectrometers IN13 and IN10 at the Institut Laue-Langevin (Grenoble, France). IN13 is characterized by an energy resolution of ΔE = 8 µeV (full-width at half-maximum, FHWH) and a large scattering vector range of $0.2 < q < 4.9$ Å^{-1} [16] and uses thermal neutrons with a wavelength of λ=2.2 Å. The instrument therefore is sensitive to macromolecular motions in a space-time window of some Å in some 0.1 ns. IN10 has a very high energy resolution of ΔE = 1 µeV FWHM, a scattering vector range of $0.5 < q < 2.0$ Å^{-1} and uses cold neutrons with a wavelength of λ=6.3 Å [16]. The instrument parameters result in an observable space-time window of some Å in some ns.

The relation between the scattering angle 2θ and the modulus of the scattering vector is $q = \frac{4\pi}{\lambda} \sin(\theta)$ for elastically scattered neutrons. Measured data were analyzed in the q^2-range from 1.6 to 3.5 Å^{-2} for IN13 and 0.7 to 3.8 Å^{-2} for IN10. The samples were oriented with an angle of 135^o with respect to the incident beam. Multiple scattering was neglected as the transmissions of all samples were larger or equal 0.9. The measured data were corrected for empty cell scattering and the neutron detectors were calibrated with a vanadium reference. The weight of the samples was measured before and after the measurements to ensure that no loss of material occurred.

2.4. X-ray diffraction

X-ray diffraction was measured on the macromolecular crystallography beamline ID14-1 at the ESRF (Grenoble, France). The beam line is optimized to measure X-ray diffraction of protein crystals, but is

also excellently suited to record powder diffraction patterns. The beamline uses monochromatic hard X-rays with a wavelength of 0.934 Å.

3. Results and Discussion

Usually, heavy water solvent is used for incoherent neutron scattering measurements of protein dynamics [17-20] as the incoherent scattering cross section of D_2O is much smaller than that of H_2O. However, as water molecules move out of the observable space-time window - some Å in some 0.1 ns for IN13 and some Å in some ns for IN10 - measurements of protein dynamics in H_2O solvent using high resolution neutron backscattering spectroscopy are feasible above ~280 K. This was already demonstrated for protein solutions in H_2O [14] and also for H_2O hydrated protein powders [21]. As D_2O has a significant influence on protein thermal stability [22] it might modify the relation of protein unfolding and amyloid formation in apo-Mb. Therefore, we chose to perform the measurements using H_2O solvent.

Apo-Mb was investigated in the native state and in a heat incubated state. Heating of native apo-Mb above 328 K is reported to result in amyloid fiber formation [6], and the extended heat incubation phase of 2 days at 338 K should lead to a saturated formation of amyloid fibers in the sample. As a control, X-ray diffraction patterns were recorded of the different samples, see Figure 1: the native state of apo-Mb before neutron scattering measurements, apo-Mb after the experiment on IN13 and the heat incubated state of apo-Mb are compared directly. The broad peaks at 0.4 - 0.8 $Å^{-1}$ and 1.1 – 2.0 $Å^{-1}$ in the X-ray diffraction pattern are typical features of globular proteins [23]. Solvent scattering contributes to the shoulder at 2.0 $Å^{-1}$ but was not subtracted from the measured intensities. The small streak at 1.54 $Å^{-1}$ is not related to scattering from the protein and might be caused by absorption of the quartz windows of the sample holders. The shift of the peak from 0.59 $Å^{-1}$ in the native state to 0.63 $Å^{-1}$ in the heated samples and the emergence of the peak at 1.33 $Å^{-1}$ are characteristic signatures of amyloid formation in apo-Mb as reported by Onai et al. [8]. Obviously, there is already a small amount of amyloid fibers present in the native state of apo-Mb, which is visible by the presence of the shoulder at 1.33 $Å^{-1}$. Larger amounts of amyloid fibers formed both during the neutron scattering experiments and by heat incubation for 2 days at 338 K, which is clearly visible by the emergence of the strong peak at 1.33 $Å^{-1}$.

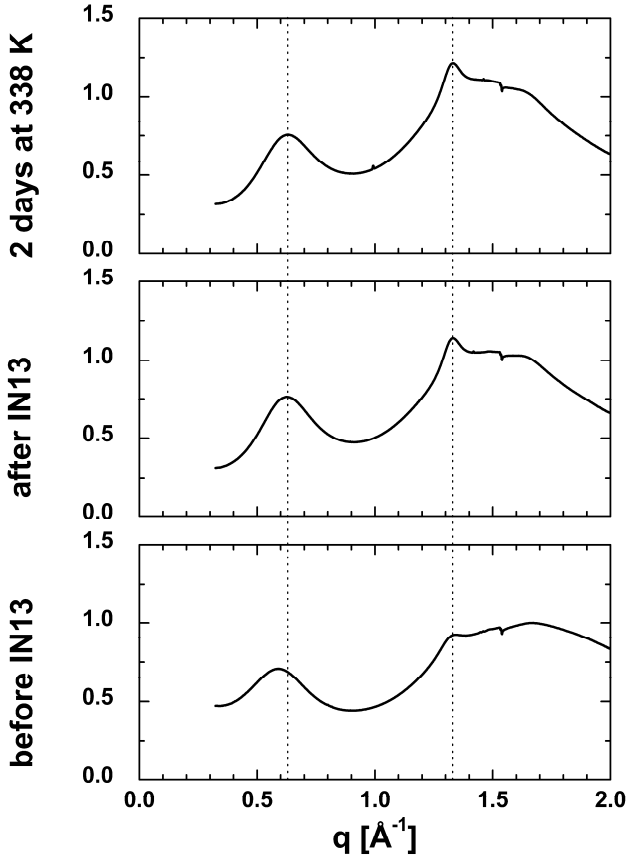

Figure 1: X-ray diffraction measured of the different samples. The shift of the broad peak from 0.59 to 0.63 Å^{-1} and the emergence of the narrow peak at 1.33 Å^{-1} are fingerprints of amyloid formation.

In the following we focus on the neutron scattering experiments. Measured elastic intensities using the neutron spectrometer IN10 are shown in Figure 2 (A) and (B), elastic data measured with the spectrometer IN13 are given in Figure 2 (C) and (D).

Mean square displacements $\langle u^2 \rangle$ were calculated from the slopes of the linear fits shown in Figure 2. The $\langle u^2 \rangle$ obtained with the IN13 spectrometer are given in Figure 3 (B), the $\langle u^2 \rangle$ determined with IN10 are reported in Figure 4 (B). In cases for which the data quality does not allow to derive sufficiently precise information about changes in the $\langle u^2 \rangle$, an analysis of the summed elastic intensity $\sum I(q)$ as a function of temperature in the same q range can give a good indication of the presence of a transition in dynamical behavior [9]. Normalized summed elastic intensities of native apo-Mb and heat incubated apo-Mb are shown in Figure 3 (A) measured with IN13 and in Figure 4 (A) measured with IN10. However, it should be noted that no information about the amplitudes of motions or about protein resilience in absolute units can be deduced from the summed elastic intensity analysis.

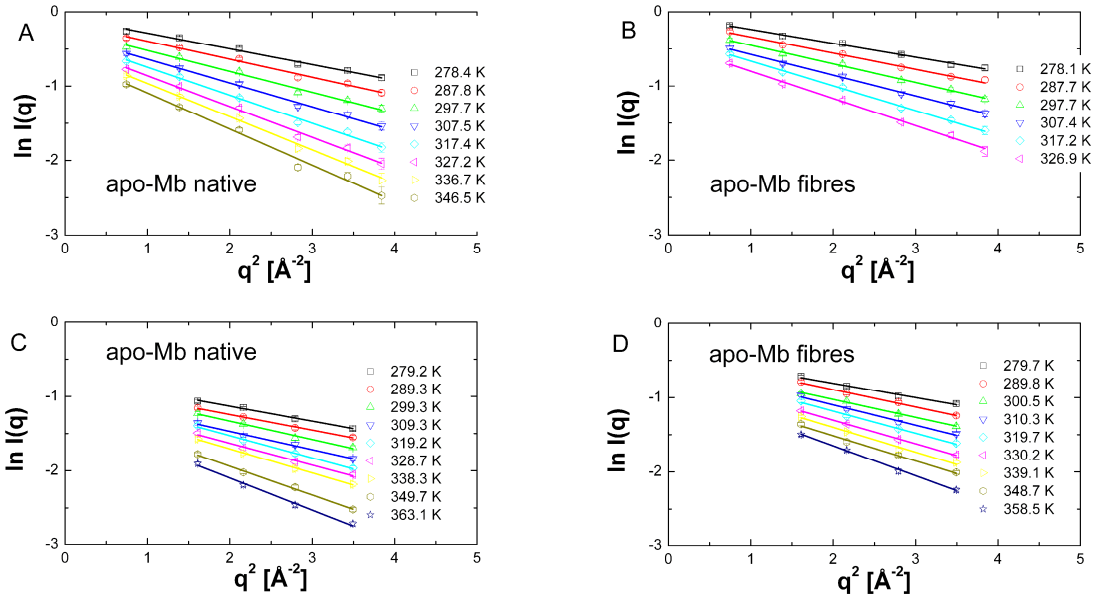

Figure 2: Measured EINS of the different samples. Data shown in A and B were measured on the instrument IN10, data in C and D were measured on IN13. Straight lines are linear fits to the data.

The transition in the dynamics of native apo-Mb at around 320 K is clearly visible in the summed elastic intensities on both instruments. The transition was observed before [9] and attributed to the change from a 'softer' α helical native structure of apo-Mb to a 'stiffer' β sheet structure in amyloid fibers. The break at 320 K is better visible in the IN10 than in the IN13 data. This seems to indicate that protein dynamics in the ns time scale depend more strongly on the secondary structure than protein dynamics in the 0.1 ns time scale. As expected, the heat incubated sample does not show any break at around 320 K, which indicates that amyloid formation has been completed during heat incubation for 2 days at 338 K.

On the other hand, the $\langle u^2 \rangle$ of the native state and of the heat incubated state measured with IN13 overlap within the error bars and no change in the dynamics of native apo-Mb at 320 K is visible. Mean force constants $\langle k' \rangle$ were derived from the $\langle u^2 \rangle$ measured with IN13 and are given in Table 1. Heat incubated apo-Mb was found to be only slightly stiffer than apo-Mb. Considering the error bars both native and heat incubated apo-Mb seem to have similar stiffness.

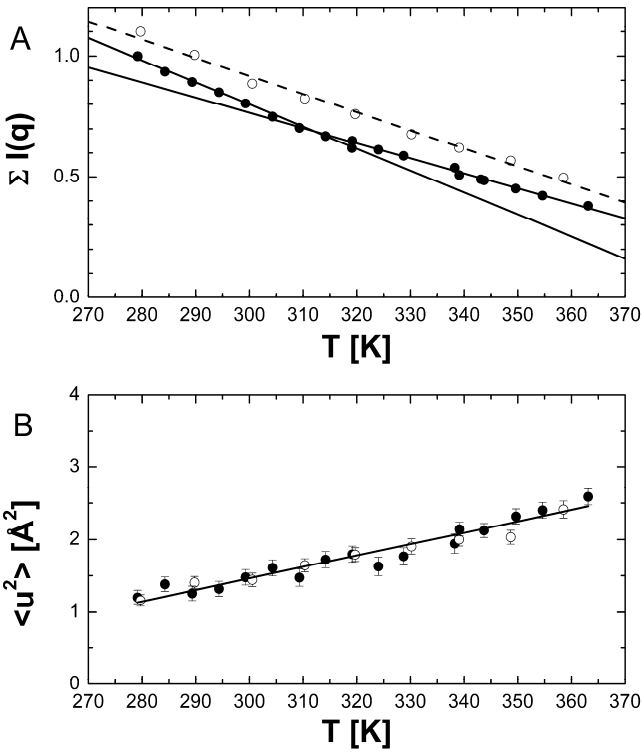

Figure 3: Native apo-Mb (filled symbols) and heat incubated apo-Mb (empty symbols) measured with IN13. (A) Summed elastic intensity $\sum I(q)$ and (B) mean square displacements $\langle u^2 \rangle$. The solid line in (B) corresponds to a linear fit to the $\langle u^2 \rangle$ of native apo-Mb.

Table 1: Effective force constants $\langle k' \rangle$ measured using the IN13 spectrometer.

Sample	**$\langle k' \rangle$ [N/m]**
Native apo-Mb	0.18 +/- 0.01
Heat incubated apo-Mb	0.20 +/- 0.01

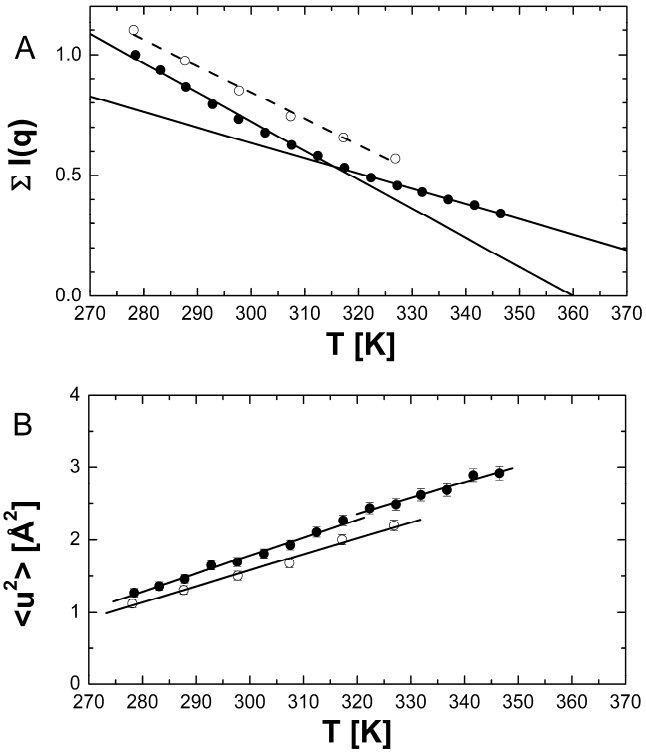

Figure 4: Native apo-Mb (filled symbols) and heat incubated apo-Mb (empty symbols measured with IN10. (A) Summed elastic intensity $\sum I(q)$ and (B) mean square displacements $\langle u^2 \rangle$.

Table 2: Effective force constants $\langle k' \rangle$ measured using the IN10 spectrometer.

Sample	**$\langle k' \rangle$ [N/m]**
Native apo-Mb T < 320 K	0.110 +/- 0.004
Native apo-Mb T > 320 K	0.126 +/- 0.012
Heat incubated apo-Mb	0.124 +/- 0.006

Comparing the $\langle u^2 \rangle$ measured with IN10, the amplitudes of motion of the heat incubated sample seem to be significantly smaller than the native state. This might indicate that thermal fluctuations in fully formed amyloid fibers are smaller than in the α helical native state. As the $\langle u^2 \rangle$ of the heat incubated apo-Mb are also smaller than the $\langle u^2 \rangle$ of native apo-Mb above 328 K, this would imply that amyloid formation in apo-Mb extends over a longer time and is not fully completed during the IN10 experiment. However, the reduced $\langle u^2 \rangle$ might also just be caused by a smaller hydration level in the heat incubated sample than in native apo-Mb. A clear break in the $\langle u^2 \rangle$ of apo-Mb at 320 K is absent. However, there might be a subtle change in the slope below and above 320 K. Effective force constants $\langle k' \rangle$ were calculated from the mean square displacements and are given in Table 2. The changes are only small but it seems to be that the α helical native state of apo-Mb below 320 K is slightly softer than the β sheet state of apo-Mb above 320 K, which is in agreement with previous results using the summed elastic intensity analysis [9]. The heat incubated apo-Mb with fully developed amyloid fibers seems to have a similar resilience as the structure of apo-Mb above 320 K.

4. Summary

We present a study on protein dynamics during amyloid formation in apo-Mb using EINS. Changes in the dynamics during the α-to-β transition of apo-Mb at 320 K in the 0.1 ns and 1 ns time-scale are clearly visible in the summed elastic intensities on both instruments. Although we have collected data with high statistics, no changes in the mean square displacements in the 0.1 ns time scale are visible during the α-to-β transition. In the ns time-time scale there might be a small change of slope in the $\langle u^2 \rangle$ during the α-to-β transition in apo-Mb. The $\langle u^2 \rangle$ of heat incubated apo-Mb seem to be reduced in the ns but not in the 0.1 ns time-scale as compared to native apo-Mb. The effective force constants determined in the ns time-scale are in agreement with a α helical structure of apo-Mb below 320 K being softer than the β sheet structure above 320 K. Heat incubated apo-Mb seems to have a similar resilience as apo-Mb above 320 K. Furthermore, our study indicates that average protein dynamics in the 0.1 ns time scale doesn't seem to be correlated strongly to the secondary structure content of proteins. Thermal fluctuations in proteins in the ns time scale seem to depend more strongly on the secondary structure of proteins.

5. Acknowledgements

The author (A.M.S.) thanks Prof. Georg Büldt for continuous support. Trevor Forsyth and Estelle Moussou are gratefully acknowledged for their help with the X-ray measurements. We also thank Moeava Tehei, Francesca Natali, and Prof. Judith Peters for fruitful discussions and help with the experiments on IN13 and IN10. This work is based on experiments performed at the ILL and at the ESRF in Grenoble, France.

References

[1] Dobson, C.M. 1999 *Trends Biochem Sci* **24** 329-332
[2] Stefani, M. and C.M. Dobson 2003 *J Mol Med* **81** 678-99
[3] Dobson, C.M. 2003 *Nature* **426** 884-90
[4] Eanes, E.D. and G.G. Glenner 1968 *J Histochem Cytochem* **16** 673-7
[5] Frauenfelder, H., B.H. McMahon, and P.W. Fenimore 2003 *Proc Natl Acad Sci U S A* **100** 8615-8617
[6] Fändrich, M., M.A. Fletcher, and C.M. Dobson 2001 *Nature* **410** 165-166
[7] Fändrich, M., et al. 2003 *Proc Natl Acad Sci U S A* **100** 15463-15468
[8] Onai, T., et al. 2007 *J Appl Crystallogr* **40** S184-S189
[9] Fabiani, E., et al. 2009 *Eur Biophys J* **38** 237-244
[10] Sears, V.F. 1992 *Neutron News* **3** 26-37
[11] Gabel, F., et al. 2002 *Q Rev Biophys* **35** 327-67
[12] Smith, J.C. 1991 *Q Rev Biophys* **24** 227-291
[13] Kidera, A. and N. Go 1990 *Proc Natl Acad Sci U S A* **87** 3718-22
[14] Tehei, M., et al. 2004 *EMBO Rep* **5** 66-70
[15] Zaccai, G. 2000 *Science* **288** 1604-1607
[16] *http://www.ill.eu/instruments-support/instruments-groups/yellowbook/*. 2010.
[17] Doster, W., S. Cusack, and W. Petry 1989 *Nature* **337** 754-6
[18] Stadler, A.M., et al. 2009 *Biophys J* **96** 5073–5081
[19] Stadler, A.M., et al. 2008 *Biophys J* **95** 5449-5461
[20] Stadler, A.M., et al. 2011 *J R Soc Interface* **8** 590-600
[21] Wood, K., et al. 2007 *Proc Natl Acad Sci U S A* **104** 18049-54
[22] Bonnete, F., D. Madern, and G. Zaccai 1994 *J Mol Biol* **244** 436-47
[23] Hirai, M., et al. 2002 *J Synchr Rad* **9** 202-205